UKAEA FUS 472

EURATOM/UKAEA Fusion

Inhomogeneous void swelling near grain boundaries in irradiated materials

S.L. Dudarev, A.A. Semenov and C.H. Woo

March 2002

EURATOM/UKAEA Fusion Association

Culham Science Centre
Abingdon
Oxfordshire
OX14 3DB
United Kingdom

Telephone: +44 1235 464181
Facsimile: +44 1235 463435

Inhomogeneous void swelling near grain boundaries in irradiated materials *

S. L. Dudarev[1], A. A. Semenov[2] and C. H. Woo[2]

[1]*EURATOM/UKAEA Fusion Association, Culham Science Centre, Oxfordshire OX14 3DB, United Kingdom*

[2]*Department of Mechanical Engineering, The Hong-Kong Polytechnic University, Hung Hom, Kowloon, Hong-Kong*

(21 February 2002)

It is shown that the treatment of inhomogeneous void swelling near grain boundaries in irradiated materials based on the rate theory by Brailsford and Bullough (1972) gives good quantitative description of all the significant experimentally observed features characterising the effect, including the formation of peaks of void swelling and denuded zones, and explains the observed shape of swelling profiles as well as the occurrence of anomalously large voids in the regions adjacent to grain boundaries.

I. INTRODUCTION

The development of mathematical models describing materials driven far from equilibrium reviewed by Martin (1998) has recently become an important element of the international programme on the development of a prototype fusion power station (Ehrlich, 1999, Eyre and Matthews, 2001). Modelling the evolution of the microstructure of a material in a hostile irradiation environment (Odette *et al*, 2001) requires investigating processes occurring simultaneously on several distinct time and length scales and establishing a link between theoretical predictions and experimental observations.

---

submitted to the Proceedings of the Royal Society (London), ser. A

On one hand, processes occurring at grain boundaries in an irradiated material play an important part in determining its stability under irradiation. This was highlighted by the recent molecular dynamics investigation of cascade effects occurring in nanocrystalline metals carried out by Samaras *et al* (2002) where it was found that a network of nanoscale grain boundaries remained stable even after crystalline order in a part of a grain was temporarily destroyed in the core of a high-energy cascade. On the other hand, by looking at how the microstructure of the material evolves in the vicinity of a grain boundary it is possible to investigate how the presence of a perturbation (in this case, a planar sink) affects the dynamics of this evolution. It is reasonable to expect that by studying how the observed quantities vary as a function of a new variable introduced into the problem (here this new variable is the distance to the grain boundary) we should be able to investigate those aspects of dynamics of microstructual evolution that cannot be addressed in the case of a spatially homogeneous system.

The unusual phenomenon of inhomogeneous void swelling occurring in the vicinity of grain boundaries under irradiation was observed experimentally in many materials, see e.g. Chen & Buttry (1981), Singh *et al* (1982), Griffits *et al* (1988), Chen *et al* (2000) and Zinkle & Singh (2000). Following the work by Foreman *et al* (1987), who concluded that the treatment of the problem based on notions of three-dimensional diffusion of defects and biased absorption of interstitials by dislocations introduced by Brailsford & Bullough (1972) and Brailsford & Bullough (1981) could not describe the observed phenomena, the grain boundary problem attracted attention of several research groups world-wide, see Trinkaus *et al* (1993), Trinkaus *et al* (1996), Dudarev (2000,2001a) and Konobeev *et al* (2000). It is currently believed that the observed enhancement of void swelling near grain boundaries is associated with one-dimensional diffusional glide of clusters of interstitial atoms formed in collision cascades. The large spatial scale characterising both the swelling profiles and denuded zones adjacent to grain boundaries (the width of these zones may be as large as ten microns, see Foreman *et al*, 1987) can be readily explained by this model (Trinkaus *et al*, 1993) as resulting from the drastic change in the statistics of collisions between mobile defects

and sinks associated with the change in the dimensionality of the problem of scattering.

The formation of mobile clusters of interstitial atoms is often observed in molecular dynamics simulations of collision cascades (Bacon *et al*, 1997, Wirth *et al*, 1997, Osetsky *et al*, 2000). These simulations show that small clusters of interstitial atoms perform one-dimensional Brownian motion in the direction parallel to their Burgers vector. It is therefore fairly natural to assume that effects associated with one-dimensional motion of clusters may be responsible for the void swelling anomalies observed near grain boundaries (Trinkaus *et al*, 1993, Trinkaus *et al*, 1996, Dudarev, 2000). At the same time, the recent discovery by Zinkle & Singh (2000) of the fact that spatially inhomogeneous void swelling occurs near grain boundaries in concentrated alloys shows that at least in some cases the treatment based on the concept of one-dimensional transport of interstitial clusters may be difficult to justify. Indeed, the presence of compositional disorder in the crystal lattice is likely to have a dramatic effect on the transport of clusters giving rise to a significant reduction of their mobility.

Furthermore, a rigorous mathematical investigation of the problem of inhomogeneous swelling carried out using the model that assumes the presence of one-dimensionally moving interstitial clusters (Dudarev, 2001b) has shown that predictions made on the basis of this model do not agree well with experimental observations.

This has stimulated the present study where we found that better agreement with experiment can be achieved using a rate theory approach (Brailsford & Bullough, 1972, Stoller & Odette, 1986, Mansur, 1987). The treatment does not require going beyond the approximation that radiation defects perform ordinary three-dimensional diffusion. The new feature of our model is that we do not assume that the density of dislocations is a quantity independent of the distance to the grain boundary. Instead, we take it as a continuous function that vanishes at the grain boundary and reaches its asymptotic bulk value at some distance away from the boundary. Our study shows that the observed relatively large spatial scale characterising the void swelling profile near a grain boundary reflects the spatial variation of the density of dislocations near the boundary. The origin of this variation of the disloca-

tion density is likely to be associated with elastic forces acting between a dislocation and a grain boundary (Bacon *et al*, 1979). This correlates well with recent dislocation dynamics simulations showing that dislocations interacting *via* long-range elastic forces form network structures on the micron scale (de la Rubia *et al*, 2000). In our work we do not study the dislocation dynamics aspect of the problem and instead attempt to restore the profile of the density of dislocations on the basis of the available experimental information on void swelling profiles.

II. THE MODEL AND ITS SOLUTION

In this section we investigate solutions of self-consistent equations describing diffusion of vacancies and interstitial atoms, and also nucleation and growth of voids in the vicinity of a grain boundary in the presence of a spatially inhomogeneous distribution of dislocation lines. We assume that the grain boundary lies in the plane $x = 0$ and that concentrations $c_v(x,t)$ and $c_i(x,t)$ of vacancies and interstitial atoms, which are functions of distance x from the boundary, satisfy the system of two equations

$$D_\alpha \frac{d^2}{dx^2} c_\alpha(x,t) + K - \left[Z_\alpha \rho(x,t) + 4\pi \int_0^t \nu(x,\tau) a(x,t,\tau) d\tau \right] D_\alpha c_\alpha(x,t) = 0, \qquad (1)$$

where index α refers to either vacancies ($\alpha = v$) or interstitials ($\alpha = i$). In equations (1) K is the effective (inclusive of recombination) rate of generation of point defects, D_v and D_i are diffusion coefficients and $\rho(x,t)$ is the density of dislocation lines. The term in square brackets is the spatial distribution of sink strengths, where $\nu(x,\tau)$ is the void nucleation rate, τ is the nucleation time and $a(x,t,\tau)$ is the radius of a void nucleated at time τ at distance x from the grain boundary. Z_i and Z_v are the dislocation bias factors (Brailsford & Bullough, 1981, Mansur, 1987). These factors describe in the mean field approximation the fact that, due to the larger formation volume of an interstitial atom defect and the resulting larger energy of its elastic interaction with a dislocation, the rate of absorption of mobile interstitials by edge dislocations is higher than the rate of absorption of vacancies. The fact

that $Z_i > Z_v$ gives rise to a positive net flux of vacancies $D_v c_v - D_i c_i > 0$ and leads to nucleation and growth of voids. Profiles of concentration of point defects considered as a function of time t are assumed to follow adiabatically the time dependence of the density of voids and dislocation lines. The grain boundary is treated as a perfect sink for both vacancies and interstitial atoms giving rise to the homogeneous boundary condition $c_v(0,t) = 0$ and $c_i(0,t) = 0$.

The growth of a void situated at a distance x from the grain boundary and nucleated at time $t = \tau$ is described by the equation (see Brailsford & Bullough, 1972)

$$\frac{da^2(x,t,\tau)}{dt} = 2\Theta(t-\tau)[D_v c_v(x,t) - D_i c_i(x,t)], \tag{2}$$

where $\Theta(t-\tau) = 1$ for $t > \tau$ and $\Theta(t-\tau) = 0$ for $t < \tau$.

In some simple cases equations (1) can be solved analytically. However, below we shall see that these simplified solutions do not correspond to cases for which experimental data are available. We therefore need to develop a numerically stable procedure suitable for finding solutions of equations (1) in the case where $\rho(x)$ is an arbitrary continuous function of the distance x between a given point and the grain boundary. The requirement that the procedure should retain stability in the limit of large x is very significant since in this limit the two linearly independent solutions of equations (1) have the form $c_\alpha \sim \exp(\pm\sqrt{\rho Z_\alpha}x)$, and the presence of the exponentially growing solution gives rise to an instability similar to those known in the treatment of reflection of waves from the surface of an absorbing medium (Dudarev, 1997).

To solve equations (1), we define a new function $\Pi(x) = D_\alpha c_\alpha(x,t)$ and the spatial distribution of sink strengths $\Omega^2(x) = Z_\alpha \rho(x,t) + 4\pi \int_0^t \nu(x,\tau) a(x,t,\tau) d\tau$. Function $\Pi(x)$ satisfies equation

$$\frac{d^2}{dx^2}\Pi(x) - \Omega^2(x)\Pi(x) = -K. \tag{3}$$

In the case $K = 0$ this equation has two linearly independent solutions $\Pi_+(x)$ and $\Pi_-(x)$ satisfying asymptotic conditions $\Pi_\pm(x) \sim \exp(\mp\Omega_\infty x)$, where $\Omega_\infty = \lim_{x\to\infty} |\Omega(x)|$. Solution

$\Pi_+(x)$ is regular in the limit $x \to \infty$ and $\Pi_-(x)$ diverges in this limit. The Wronskian $W(x) = \Pi_-(x)[d\Pi_+(x)/dx] - \Pi_+(x)[d\Pi_-(x)/dx]$ of these two solutions is a quantity that is independent of x for any continuous distribution of sink strengths $\Omega^2(x)$. Indeed, by differentiating $W(x)$ we arrive at the equation

$$\frac{d}{dx}W(x) = \left[\frac{d^2}{dx^2}\Pi_+(x)\right]\Pi_-(x) - \left[\frac{d^2}{dx^2}\Pi_-(x)\right]\Pi_+(x)$$
$$= \Omega^2(x)\Pi_+(x)\Pi_-(x) - \Omega^2(x)\Pi_-(x)\Pi_+(x) = 0,$$

which proves that $W(x) = const$ for any continuous function $\Omega^2(x)$.

Let us now look for a solution of the *inhomogeneous* equation (3). Using the above property of the Wronskian, we observe that the following combination of solutions $\Pi_+(x)$ and $\Pi_-(x)$ of the *homogeneous* equation (3)

$$\tilde{\Pi}(x) = -\frac{\Pi_-(0)}{\Pi_+(0)}\Pi_+(x)\int_0^\infty \Pi_+(x')dx' + \Pi_+(x)\int_0^x \Pi_-(x')dx' + \Pi_-(x)\int_x^\infty \Pi_+(x')dx', \qquad (4)$$

satisfies the necessary boundary condition $\tilde{\Pi}(0) = 0$. Furthermore, by substituting this solution into (3) we find that $d^2\tilde{\Pi}(x)/dx^2 - \Omega^2(x)\tilde{\Pi}(x) = W(x)$. Taking into account the fact that $W(x) = const$ we see that equation (3) can be satisfied if we choose the normalisation of functions $\Pi_+(x)$ and $\Pi_-(x)$ in such a way that $W(x) = -K$.

The two solutions $\Pi_+(x)$ and $\Pi_-(x)$ of the homogeneous equation (3) that are required in order to construct (4) can be found using the R-matrix algorithm (Dudarev, 1997), the details of which are given in Appendix A. This completes the mathematical procedure that we now apply to finding profiles of concentration of interstitial atoms and vacancies in the vicinity of a grain boundary in the presence of inhomogeneously distributed dislocations.

Figures 1 and 2 show profiles of concentration calculated using the method described above for a step-like (Fig.1) and for an arbitrary continuous (Fig.2) distribution of the density of dislocations. These figures show that changes in the shape of the profile of density of dislocations $\rho(x)$ have a substantial effect on the form of solutions of equations (1). In the case of a step-like function $\rho(x)$ shown in Fig.1 the net flux of vacancies to voids varies linearly as a function of x in the dislocation-free zone. This agrees fully with the analytical

solution of the problem given in Appendix B. On the other hand, in the case where $\rho(x)$ is described by a smooth function of variable x (see Fig.2), the shape of the net vacancy flux profile depends on the distribution of the density of dislocations in a more complex way that is difficult to describe using analytical approximations.

Further study of kinetics of inhomogeneous swelling requires introducing a model describing the nucleation and growth of voids. Experimental data discussed in previous publications by Foreman *et al* (1987), Dudarev (2000), Dudarev (2001b) correspond to relatively low irradiation doses where voids continue to nucleate over the entire period of observations. The data described by Foreman *et al* (1987) show that the concentration of voids increases nearly linearly with the irradiation dose. This suggests that in the interval of irradiation doses investigated by Foreman *et al* (1987) nucleation is almost unaffected by the presence of existing voids. Moreover, since the observed nucleation rate remains relatively high over the interval of doses studied experimentally, we can assume that thermal emission of vacancies from voids does not significantly influence the nucleation process or, in other words, the critical radius of voids remains small. In this case we may consider the process of nucleation as Brownian motion of the population of voids in the void size space, where nucleation and growth is driven by net flux of vacancies to voids $D_v c_v - D_i c_i$ competing against random fluctuations of fluxes of vacancies and interstitials. Taking into account the fact that the amplitude of fluctuations of fluxes of point defects is proportional to $D_v c_v + D_i c_i$ (see Semenov & Woo (1999) for more detail), we find that the rate of nucleation of voids is given by (Semenov & Woo, 2002)

$$\nu(x,t) = \mathcal{R}K \frac{D_v c_v(x,t) - D_i c_i(x,t)}{D_v c_v(x,t) + D_i c_i(x,t)}, \tag{5}$$

where $\mathcal{R}$ is a rate factor that is assumed to remain constant over the interval of irradiation doses studied experimentally.

We now investigate self-consistent solutions of equations (1), (2), (4) and (5) and study the evolution of the spatially inhomogeneous distribution of voids nucleating and growing in the vicinity of a grain boundary.

III. RESULTS AND DISCUSSION

The purpose of this study of non-linear equations (1)-(5) is to find out whether or not the rate theory can be applied to the treatment of the problem of inhomogeneous void swelling near a grain boundary and whether a plausible theoretical argument can be put forward within the rate theory in order to explain the key experimentally observed features characterising the effect.

We start by summarising the experimental findings. There are several significant features characterising the phenomenon of inhomogeneous swelling that a suitable theoretical model should be able to address. They are (i) the relatively large spatial scale of profiles of inhomogeneous void swelling, (ii) the occurrence of void denuded zones in the regions adjacent to grain boundaries (see Fig. 3 from the paper by Singh *et al*, 1982), (iii) the nearly symmetric shape of void swelling peaks (this point is particularly difficult to address within the existing theoretical approach, see Dudarev, 2001b) and (iv) the origin of unusually large voids often observed close to grain boundaries in the void denuded zones (these large voids can be clearly seen in Fig. 3 by Chen & Buttry,1981, and in Fig.3 by Singh *et al*, 1982). We should also note that in some cases peaks of void swelling were not observed at all (Norris, 1971) and the spatial scale characterising the effect was fairly small.

We begin by arguing that the assumption that the density of dislocation lines can be approximated by a function independent of the distance to the boundary does not necessarily represent a good starting point for the treatment of the problem. Indeed, the presence of image forces acting between a grain boundary and a dislocation (see, e.g. Bacon *et al* (1979) for a comprehensive review of the subject) should inevitably lead to the formation of zones denuded of *dislocations* in the vicinity of grain boundaries in well annealed materials (note that experimental data reported by Foreman *et al* (1987) were obtained using well annealed samples). It is therefore natural to treat the problem starting from a profile of the density of dislocations $\rho(x)$, where function $\rho(x)$ vanishes at $x = 0$ in order to minimise the elastic energy of interaction between the dislocations and the grain boundary, and where $\rho(x)$

reaches its asymptotic bulk value at a certain distance away from the grain boundary. It is also reasonable to assume that the overall density of dislocation lines should increase under irradiation and that dislocation climb would give rise to the propagation of dislocations from the interior of the grain towards grain boundaries.

Following these arguments, we approximate the density of dislocation lines by a simple analytical formula

$$\rho(x,t) = \rho_0(t)\frac{\exp(-w/x)}{1+\exp[-(x-x_0(t))/w]}, \tag{6}$$

where $\rho_0(t)$ and $x_0(t)$ are slowly varying functions of irradiation time. The function given by equation (6) vanishes rapidly in the limit $x \to 0$ and reaches its bulk asymptotic value $\rho(x) \to \rho_0(t)$ in the limit $x \to \infty$. The irradiation time t is related to the dose ϕ *via* $\phi = Kt$.

Figure 3 shows the distribution of the volume density of voids calculated for the three values of irradiation dose for which experimentally observed values were reported by Foreman *et al* (1987). The incubation dose corresponding to the onset of growth is assumed to be equal to 0.08 dpa. Values of the density of voids at swelling peaks observed experimentally were $N_v^{(\phi=0.13dpa)} = 5.5$ micron^{-3}, $N_v^{(\phi=0.26dpa)} = 16$ micron^{-3} and $N_v^{(\phi=0.65dpa)} = 30$ micron^{-3}. These values agree reasonably well with the calculated values $N_v^{(\phi=0.13dpa)} = 3$ micron^{-3}, $N_v^{(\phi=0.26dpa)} = 10$ micron^{-3} and $N_v^{(\phi=0.65dpa)} = 28$ micron^{-3} representing void densities at distances corresponding to peaks of void swelling profiles shown in Figure 5 and discussed below.

Profiles of the density of dislocations (6) are assumed to evolve with irradiation dose as shown in Figure 4. The density of dislocations vanishes close to the grain boundary and this makes it possible to avoid gaining a large contribution to the elastic energy of the system associated with the interaction between dislocations and the grain boundary. The force acting on a single straight dislocation situated at a distance x from the boundary varies with the distance as (Bacon *et al*, 1979)

$$F = -\frac{E^{(1-2)} - E^{(1)}}{x}, \tag{7}$$

where $E^{(1)}$ is the energy of the dislocation in an infinite crystal and $E^{(1-2)}$ is the energy of the same dislocation at the boundary between the two grains 1 and 2. The fact that formula (7) diverges in the limit of small x shows that the formation of dislocation denuded zones near grain boundaries is likely to occur irrespectively of whether the interaction is repulsive or attractive.

Given the overall functional form of the dislocation density profile (6), the parameters x_0, w and the rate of increase of the asymptotic bulk density of dislocations $\rho_0(t)$ have been chosen to reproduce the experimentally observed profiles of void swelling shown in Figure 5. The comparison of calculated and observed profiles shows that using the present model it is possible to achieve good agreement with experimental data both in terms of the shape of the profiles and also in terms of the agreement between the calculated and observed values of void swelling corresponding to the interior region of the grain. None of this was possible within the framework of models considered previously (Dudarev, 2000, Dudarev, 2001b).

A particularly important feature characterising the effect of inhomogeneous void swelling is the occurrence of unusually large voids in the void denuded zones adjacent to grain boundaries. The rarely distributed large voids situated very close to grain boundaries can be seen in electron microscope images obtained by Chen & Buttry (1981) and by Singh *et al* (1982). So far none of the existing models was able to account for the fact that the rate of growth of voids would be higher in the regions where the nucleation of voids is suppressed. Figure 6 shows how this phenomenon can be explained using the model described above. The average radius $\langle a \rangle$ of a void is a quantity that is related the local value of void swelling S_v and the local density of voids N_v, namely

$$S_v = \frac{4}{3}\pi N_v (\langle a \rangle)^3.$$

A comparison of profiles shown in Figures 3 and 5 shows that a substantial part of each swelling peak is situated in the region where the density of voids is low. The fact that values of local swelling still remain high where the density of voids is low shows that the average size of voids in these regions can be several times greater than the size of voids growing in

the interior of the grain. The occurrence of large voids in the vicinity of grain boundaries is associated with the low density of sinks in the regions adjacent to the boundaries and the resulting high local values of the net vacancy flux $D_v c_v - D_i c_i$. Figure 7 illustrates this point in more detail.

It is interesting to compare results obtained in the present study with the investigation of radiation damage in aluminium performed by Mazey *et al* (1976). The authors found that the rate theory treatment was able to describe void swelling in pure aluminium over a large interval of irradiation doses. The swelling rates were found to be sensitive to the purity of the material, increasing dramatically for the purest samples. Still, even for the very pure samples the swelling rates reported in by Mazey *et al* (1976) were significantly lower than those described by Foreman *et al* (1987). For example, for the 99.9999% purity aluminium the highest value of swelling found for the irradiation dose of 0.65 dpa was $S_v = 0.15\%$ (see Fig.6 by Mazey *et al*, 1976), while Foreman *et al* (1987) quotes a much higher value of $S_v = 0.8\%$ for the case of swelling in the interior region of the grain at the same irradiation dose. Taking into account the presence of continuous nucleation that occurred in experiments described by Foreman *et al* (1987), we find that significantly higher values of bias factors ($Z_i - Z_v \approx 22\%$) were required in order to reproduce the data given by Foreman *et al* (1987) in comparison with the data given by Mazey *et al* (1976).

The model considered above makes it possible to comment on cases where the effect of inhomogeneous void swelling near grain boundaries was *not* observed, see e.g. the work by Norris (1971). We found above that the formation of dislocation denuded zones near grain boundaries prior to irradiation is a necessary precondition that needs to be satisfied in order to obtain a peak of void swelling situated at a certain distance away from the grain boundary. It is known that the type of the dislocation network existing in a given material depends entirely on the way the material is treated before irradiation. In the case where the distribution of the density of dislocations is homogeneous across the grain, no peaks of void swelling are expected to occur, and this may explain their absence in experiments performed by Norris (1971).

In summary, we would like to emphasise the phenomenological nature of the study described in this paper. The model proves to be capable of describing the experimentally observed phenomenon of inhomogeneous void swelling in a somewhat better and more comprehensive way than other models currently available in the literature. The model shows that the effect of formation of profiles of spatially inhomogeneous void swelling may be associated with the inhomogeneity in the distribution of dislocations near a grain boundary. This main result of the present paper clearly demonstrates that the spatial distribution of the dislocation component of microstructure plays a determining part in the formation of the distribution of voids. Without a proper investigation of the evolution of the dislocation network it is difficult to draw conclusions about the real physical cause of the large-scale spatial inhomogeneity of the void swelling profile in the vicinity of a grain boundary.

Here, no attempt has been made here to describe the observed effects by starting from first principles and by considering elementary acts of formation of interstitial loops in collision cascades and the interaction of defects with the dislocation network. A more detailed investigation of the problem would require using a multiscale approach linking simulations that describe microstructural evolution on atomistic and mesoscopic scales. Methods reviewed recently by Odette *et al* (2001) may help in addressing this issue.

IV. ACKNOWLEDGMENTS

This work was performed as a part of a collaborative programme on modelling fusion materials sponsored by the International Energy Agency (IEA). We would like to acknowledge stimulating discussions with Prof. R. Bullough FRS and Prof. A. P. Sutton, and would like to thank Dr. Ian Cook for encouragement and valuable comment. Work at the Hong-Kong Polytechnic University was supported by University Grants G-T007 and G-T238, and also by grant PolyU 5167/01E awarded by the Hong-Kong Research Grant Council. Work at the UKAEA Culham Science Centre was funded by the UK Department of Trade and Industry and by EURATOM.

V. APPENDIX A

In this appendix we describe a numerical approach to solving equations (3) and (4). We assume that we need to find these solutions on an interval $[0, L]$, where L is sufficiently large, so that $L\Omega_\infty \gg 1$. We split the entire interval of integration into $N \gg 1$ slices of equal length $l = L/N$. Within each slice function $\Omega^2(x)$ can be approximated by its value corresponding to the middle of the slice, so that for $x_i < x < x_{i+1}$ we have

$$\frac{d^2}{dx^2}\Pi(x) - \Omega_i^2\Pi(x) = 0, \tag{8}$$

where $\Omega_i^2 = \Omega^2([x_i + x_{i+1}]/2)$ and $x_N = L$. Function $\Omega^2(x)$ is now approximated by a discontinuous set of step-like segments. The solution of equation (8) is a function that is continuous and differentiable everywhere on the interval $[0, L]$. Values of the derivative $d\Pi/dx$ and the solution $\Pi(x)$ at both sides of every slice $[x_i, x_{i+1}]$ are related *via*

$$\begin{aligned} \frac{d\Pi(x)}{dx}\Big|_{x_i} &= \cosh(\Omega_i l)\frac{d\Pi(x)}{dx}\Big|_{x_{i+1}} + \Omega_i \sinh(\Omega_i l)\Pi(x_{i+1}) \\ \Pi(x_i) &= \frac{\sinh(\Omega_i l)}{\Omega_i}\frac{d\Pi}{dx}\Big|_{x_{i+1}} + \cosh(\Omega_i l)\Pi(x_{i+1}). \end{aligned} \tag{9}$$

Introducing the R-matrix by the relation $R_i = d\ln[\Pi(x)]/dx\Big|_{x_i}$ and using equation (9), we find

$$R_{i+1} = \frac{\cosh(\Omega_i l)R_i + \Omega_i \sinh(\Omega_i l)}{\cosh(\Omega_i l) + \Omega_i^{-1}\sinh(\Omega_i l)R_i}, \tag{10}$$

or, *vice versa*,

$$R_i = \frac{\cosh(\Omega_i l)R_{i+1} - \Omega_i \sinh(\Omega_i l)}{\cosh(\Omega_i l) - \Omega_i^{-1}\sinh(\Omega_i l)R_{i+1}}. \tag{11}$$

In the limit $x \to \infty$ we retain only the solution that falls off exponentially as a function of coordinate x. This corresponds to the boundary condition

$$R_N = -\Omega_\infty. \tag{12}$$

Using this boundary condition and equation (11), we find values R_{N-1}, R_{N-2} ... R_0. Solution $\Pi_+(x)$ that remains regular in the limit $x \to \infty$ can now be found recursively as

$$\Pi_+(x_{i+1}) = [\cosh(\Omega_i l) - \Omega_i^{-1}\sinh(\Omega_i l)R_{i+1}]^{-1}\Pi_+(x_i). \tag{13}$$

Boundary condition for $\Pi_+(x)$ at $x = 0$ is $\Pi_+(0) = 1$.

Finding solution $\Pi_-(x)$ is somewhat more difficult. We choose the boundary condition on the *derivative* of $\Pi_-(x)$ at $x = 0$ in the form $d\ln[\Pi_-(x)]/dx\Big|_{x=0} = -R_0$, where R_0 equals the boundary value of the R-matrix found previously from equations (11) and (12). We now impose the requirement following from equation (4) that the Wronskian of solutions $\Pi_-(x)$ and $\Pi_+(x)$ must be equal to $-K$. We write

$$\Pi_-(0)\frac{d\Pi_+(x)}{dx}\Big|_{x=0} - \Pi_+(0)\frac{d\Pi_-(x)}{dx}\Big|_{x=0} = -K. \tag{14}$$

Taking into account that $\Pi_+(0) = 1$, from (14) we obtain the boundary condition on $\Pi_-(x)$

$$\Pi_-(0) = K\left[d\ln[\Pi_-(x)]/dx\Big|_{x=0} - d\ln[\Pi_+(x)]/dx\Big|_{x=0}\right]^{-1}. \tag{15}$$

Now values $\Pi_-(x_1)$, $\Pi_-(x_2)$,...,$\Pi_-(x_N)$ can be found using equation (13). Finally, we write solution (4) in the form

$$\tilde{\Pi}(x) = -\frac{\Pi_-(0)}{\Pi_+(0)}\Pi_+(x)\int_0^\infty \Pi_+(x')dx' + \Pi_+(x)\Pi_-(x)\left(\int_0^x \frac{\Pi_-(x')}{\Pi_-(x)}dx' + \int_x^\infty \frac{\Pi_+(x')}{\Pi_+(x)}dx'\right), \tag{16}$$

that contains no exponentially divergent terms and provides a convenient numerical representation of function $\tilde{\Pi}(x)$.

VI. APPENDIX B

In the case of a step-like distribution of the density of dislocations equation (3) has the form

$$\frac{d^2}{dx^2}\Pi(x) + K - \rho Z\Pi(x)\Theta(x - x_0) = 0. \tag{17}$$

In the interval $0 < x < x_0$ this equation has solution $\Pi(x) = -Kx^2/2 + Ax + B$. For $x > x_0$ the solution is $\Pi(x) = (K/Z\rho) + C\exp(-\sqrt{\rho Z}x)$. Using the boundary condition $\Pi(0) = 0$ we find that $B = 0$. Conditions of continuity of the solution and its first derivative at $x = x_0$

give rise to two more equations, using which it is possible to find constants A and C. By carrying out calculations, we arrive at

$$\Pi(x) = -\frac{Kx^2}{2} + \frac{x}{x_0}\left[\left(\frac{Kx_0^2}{2} + \frac{K}{\rho Z}\right) + \left(\frac{Kx_0^2}{2} - \frac{K}{\rho Z}\right)\left(1 + x_0\sqrt{\rho Z}\right)^{-1}\right], \tag{18}$$

for $0 < x < x_0$, and

$$\Pi(x) = \frac{K}{\rho Z} + \left(\frac{Kx_0^2}{2} - \frac{K}{\rho Z}\right)\left(1 + x_0\sqrt{\rho Z}\right)^{-1} \exp\left[-\sqrt{\rho Z}(x - x_0)\right], \tag{19}$$

for $x > x_0$. In the case shown in Figure 1 this solution is indistinguishable from the solution found using the numerical algorithm described in Appendix A.

VII. REFERENCES

Bacon, D. J., Barnett, D. M. and Scattergood, R. O. 1979 Anisotropic continuum theory of lattice defects. *Prog. Mater. Sci.* **23**, 51-262

Bacon, D. J., Calder, A. F. and Gao, F. 1997 Defect production due to displacement cascades in metals as revealed by computer simulations. *Journ. Nucl. Mater.* **251**, 1-12

Brailsford, A. D. and Bullough, R. 1972 The rate theory of swelling due to void growth in irradiated metals. *Journ. Nucl. Mater.* **44**, 121-135.

Brailsford, A. D. and Bullough, R. 1981 The theory of sink strengths. *Philos. Trans. R. Soc. London*, Ser. **A302**, 87-137.

Chen, C. W., and Buttry, R. W. 1981 Void formation and denudation in ion-irradiated nickel. *Rad. Effects* **56**, 219-228

Chen, J., Jung P. and Trinkaus, H. 2000 Microstructural evolution of helium-implanted α-SiC. *Phys. Rev.* **B61**, 12923-12932

de la Rubia, T. D., Zbib, H., Khraishi, T. A., Wirth, B. D., Victoria, M. and Caturla, M. J. 2000 Multiscale modelling of plastic flow localisation in irradiated materials. *Nature* **406**, 871-874

Dudarev, S. L. 1997 Incoherent scattering of electrons by a crystal surface. *Micron* **28**, 139-158

Dudarev, S. L. 2000 Inhomogeneous nucleation and growth of cavities in irradiated materials. *Phys. Rev.* **B62**, 9325-9337

Dudarev, S. L. 2001a Effect of microstructure on the saturation of swelling in irradiated materials. *J. Phys. Condens. Matter* **13**, L9-L16

Dudarev S. L. 2001b Inhomogeneous swelling near grain boundaries in irradiated materials: cavity nucleation and growth saturation effects. In: *Microstructural Processes in Irradiated Materials - 2000*, eds. G. E. Lucas, L. L. Snead, M. A. Kirk and R. G. Elliman, Mater. Res. Soc. Symp. Proc. vol. 650 (Warrendale, PA) pp. R1.4.1-R1.4.6

Ehrlich, K. 1999 The development of structural materials for fusion reactors. *Philos. Trans. R. Soc. London*, Ser. A**357**, 595-623

Eyre, B. L. and Matthews, J. R. 2001 Materials for the power industry. *MRS Bulletin* **26**, 547-554

Foreman, A. J. E., Singh B. N. and Horsewell, A. 1987 Diffusion mechanisms for enhanced vacancy accumulation near planar sinks. *Mater. Sci. Forum* **15-18**, 895-900.

Griffiths, M., Gilbert R. W. and Coleman, C. E. 1988 Grain boundary sinks in neutron-irradiated Zr and Zr alloys. *Journ. Nucl. Mater.* **159**, 405-416

Konobeev, Yu. V., Pechenkin V. A. and Garner, F. A. 2000 Internal stress in the void denuded zone formed under HVEM irradiation of metals. in: *19th Intern. Sym. on Effects of Radiation on Materials*, American Society for Testing and Materials Symp. Proc. vol. 1366, ed. M. L. Hamilton, A. S. Kumar, S. Rosinski and M. L. Grossbeck (West Conshohocken, PA) pp. 699-712

Mansur, L. K. 1987 Mechanisms and kinetics of radiation effects in metals and alloys. In:

Kinetics of Inhomogeneous Processes, ed. G. R. Freeman (Wiley, New York) chapter 8

Martin, G. 1998 Modelling materials driven far from equilibrium. *Curr. Opinion Sol. State Mater. Sci.* **3**, 552-557.

Mazey, D. J., Bullough, R. and Brailsford, A. D. 1976 Observation and analysis of damage structure in Al and Al/Mg(N4) alloy after irradiation with 100 and 400 keV aluminium ions. *Journ. Nucl. Mater.* **62**, 73-88

Norris, D. I. R. 1971 The use of the high-voltage electron microscope to simulate fast neutron-induced void swelling in metals. *Journ. Nucl. Mater.* **40**, 66-76

Odette, G. R., Wirth, B. D., Bacon D. J. and Ghoniem, N. M. 2001 Multiscale multiphysics modelling of radiation damaged materials: embrittlement of pressure-vessel steels. *MRS Bulletin* **26**, 176-181

Osetsky, Yu. N., Bacon, D. J., Serra, A., Singh B. N. and Golubov, S. I. 2000 Stability and mobility of defect clusters and dislocation loops in metals. *Journ. Nucl. Mater.* **276**, 65-77

Samaras, M., Derlet, P. M., Van Swygenhoven, H. and Victoria, M. 2002 Computer simulation of displacement cascades in nanocrystalline Ni. *Phys. Rev. Lett.* (2002) in press

Semenov, A. A. and Woo, C. H. 1999 Applicability of the conventional master equation for the description of microstructural evolution under cascade-producing irradiation. *Appl. Phys.* **A69**, 445-451

Semenov, A. A. and Woo, C. H. 2002 Void nucleation at elevated temperatures under cascade-damage irradiation. *Appl. Phys.* to be published

Singh, B. N., Leffers, T., Green W. V. and Green, S. L. 1982 Formation of cavities at and away from grain boundaries during 600 MeV proton irradiation *Journ. Nucl. Mater.* **105**, 1-10

Stoller, R. E. and Odette, G. R. 1986 Microstructural evolution of an austenitic stainless steel fusion reactor first wall. *Journ. Nucl. Mater.* **141**, 647-653

Trinkaus, H., Singh B. N. and Foreman, A. J. E. 1993 Impact of glissile interstitial loop production in cascades on defect accumulation in the transient. *Journ. Nucl. Mater.* **206**, 200-211

Trinkaus, H., Singh B. N. and Victoria, M. 1996 Microstructural evolution adjacent to grain boundaries under cascade damage conditions and helium production. *Journ. Nucl. Mater.* **233-237**, 1089-1095.

Wirth, B. D., Odette, G. R., Maroudas D. and Lucas, G. E. 1997 Energetics of formation and migration of self-interstitials and self-interstitial clusters in α-iron. *Journ. Nucl. Mater.* **244**, 185-194

Zinkle, S. J. and Singh, B. N. 2000 Microstructure of Cu-Ni alloys neutron irradiated at 210°C and 420°C to 14 dpa. *Journ. Nucl. Mater.* **283-287**, 306-312

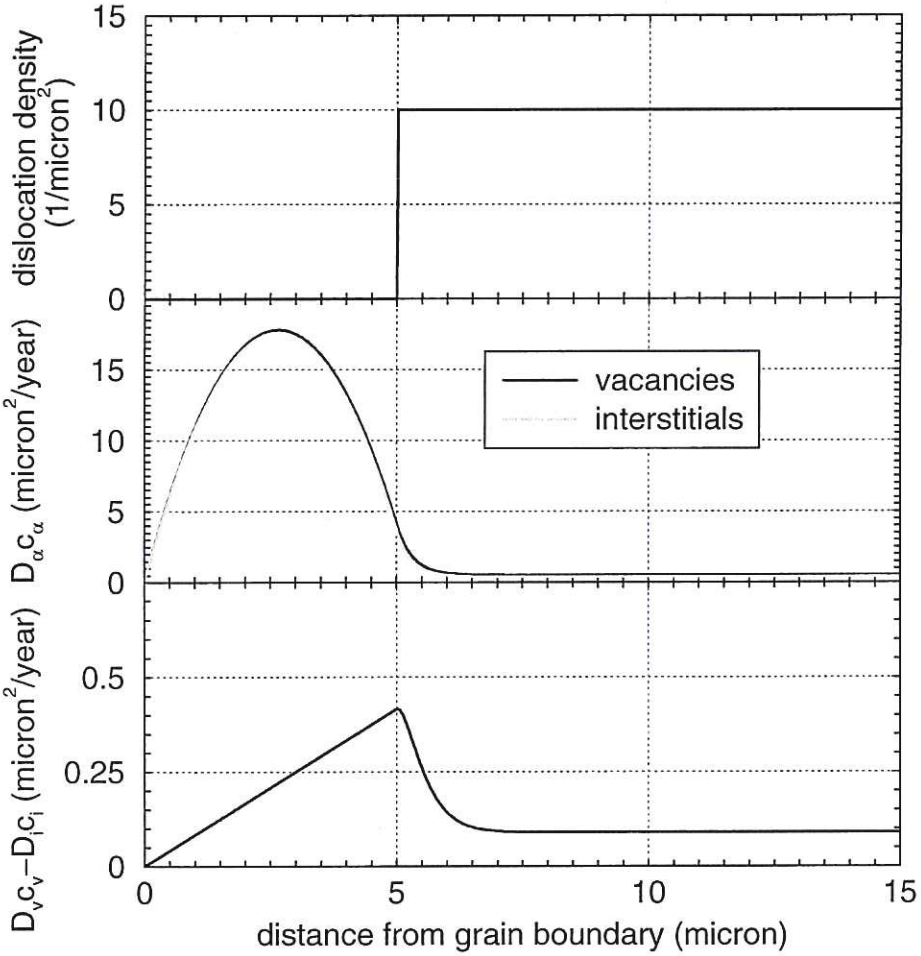

FIG. 1. Solutions of equations (1) found numerically using the R-matrix method described in Appendix A for a step-like distribution of the density of dislocations $\rho(x)$. The profile of net flux of vacancies to voids $D_v c_v(x) - D_i c_i(x)$ shown in this figure is indistinguishable from that found by an analytical calculation described in Appendix B. Bias factors used in the calculation are $Z_i = 1.22$ and $Z_v = 1.0$. The dose rate K equals 5 dpa/year.

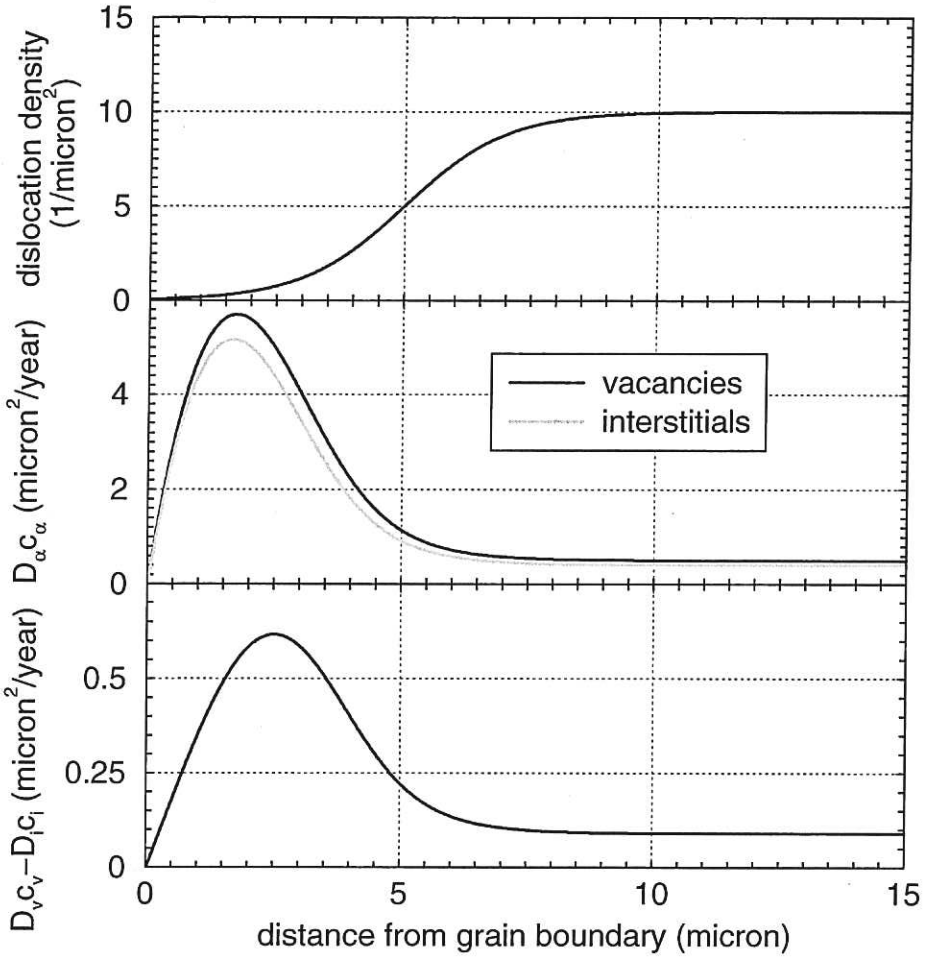

FIG. 2. Solutions of equations (1) found numerically using the R-matrix method described in Appendix A for a smooth but otherwise arbitrarily chosen distribution of the density of dislocations $\rho(x)$. The asymptotic bulk value of the density of dislocation lines, the bias factors and the dose rate remain the same as those shown in Figure 1. Note that the maximum value of function $D_v c_v - D_i c_i$ shown in this figure is greater than the maximum value of the same function calculated for a step-like distribution of the density of dislocations shown in Figure 1.

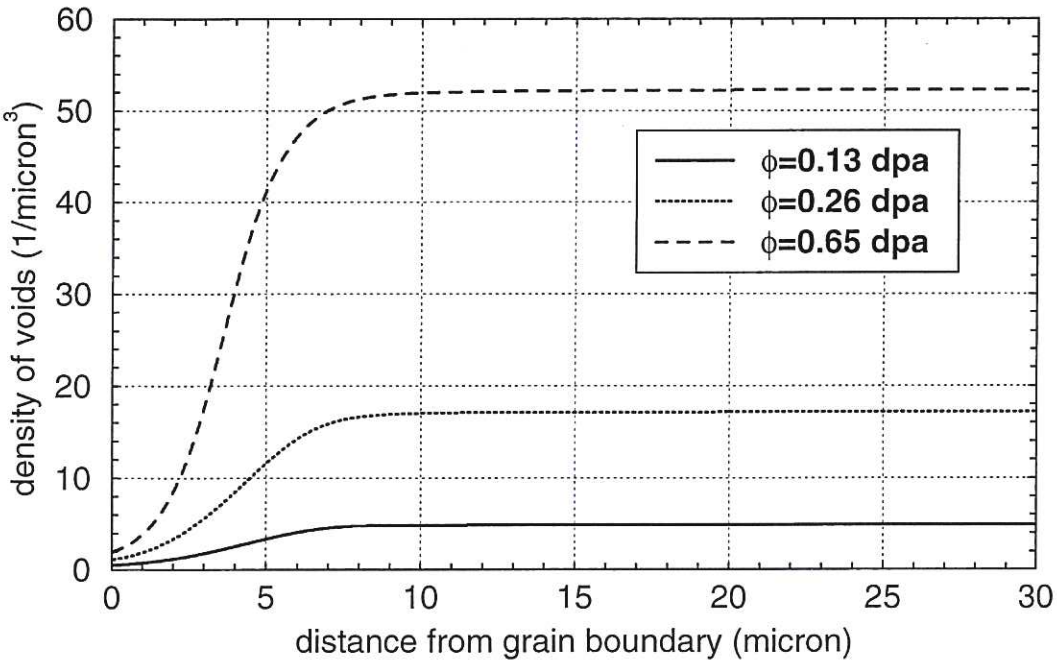

FIG. 3. Density of voids evaluated self-consistently using equations (1), (4) and (5) for $\mathcal{R} = 10^3$ micron^{-3}dpa^{-1}. Profiles shown in this figure were calculated for the three values of the irradiation dose corresponding to experimental data given by Foreman *et al* (1987). The density of voids drops by more than an order of magnitude in the region adjacent to the grain boundary resulting in the formation of a void denuded zone. Dislocation bias parameters used in calculations are $Z_i = 1.22$ and $Z_v = 1.0$

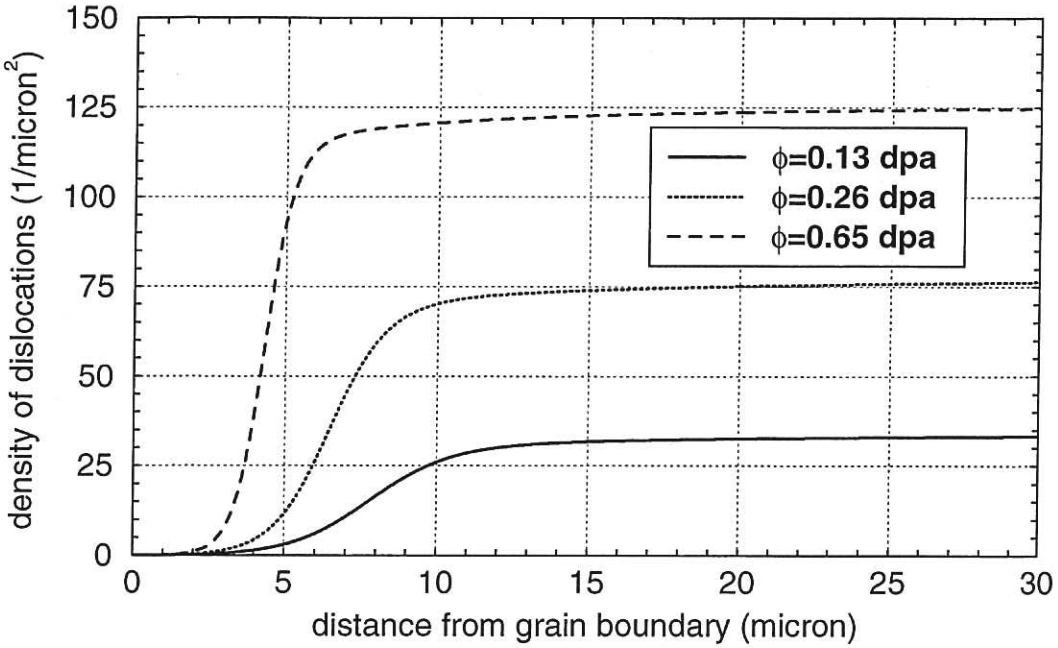

FIG. 4. Snapshots of profiles of the density of dislocation lines used in the study of solutions of equations (1). The profiles are described by the analytical expression (6), where the width of the transition region w, the distance between the centre of the transition region x_0 and the grain boundary, and the asymptotic bulk value of the dislocation density ρ_0 were assumed to vary slowly as a function of the irradiation dose.

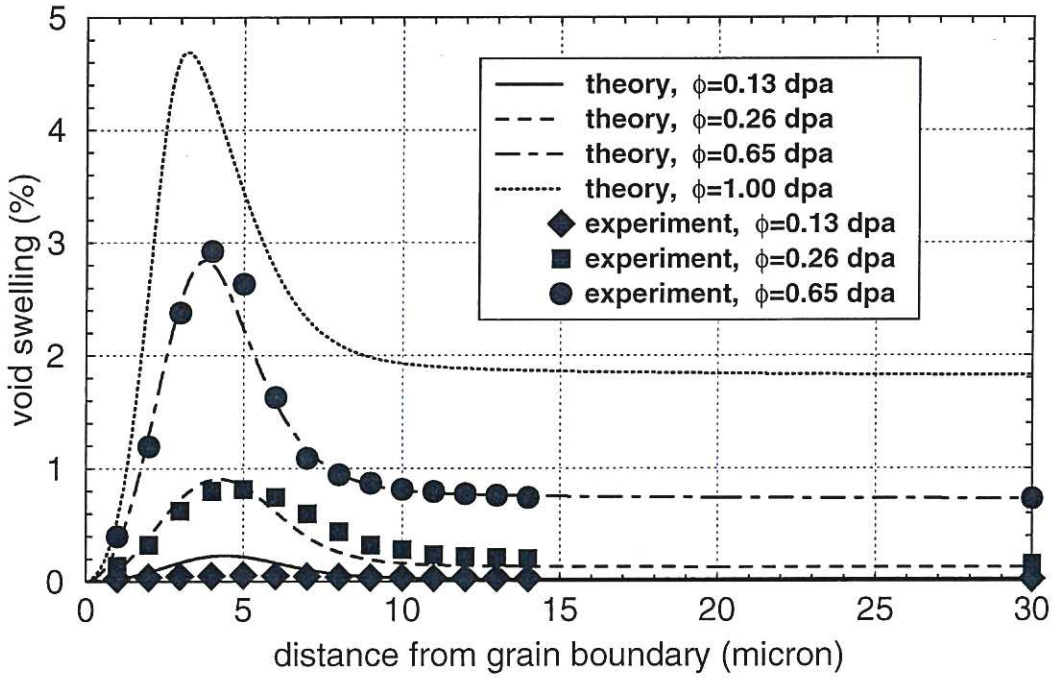

FIG. 5. Profiles of void swelling calculated numerically using self-consistent equations (1)-(5) for the three values of the total irradiation dose where experimental data are available (Foreman *et al*, 1987), and also for a somewhat larger value of the dose illustrating the absence of the immediate saturation of void swelling exhibited by the model. Bias factors used in the calculations are $Z_i = 1.22$ and $Z_v = 1.0$.

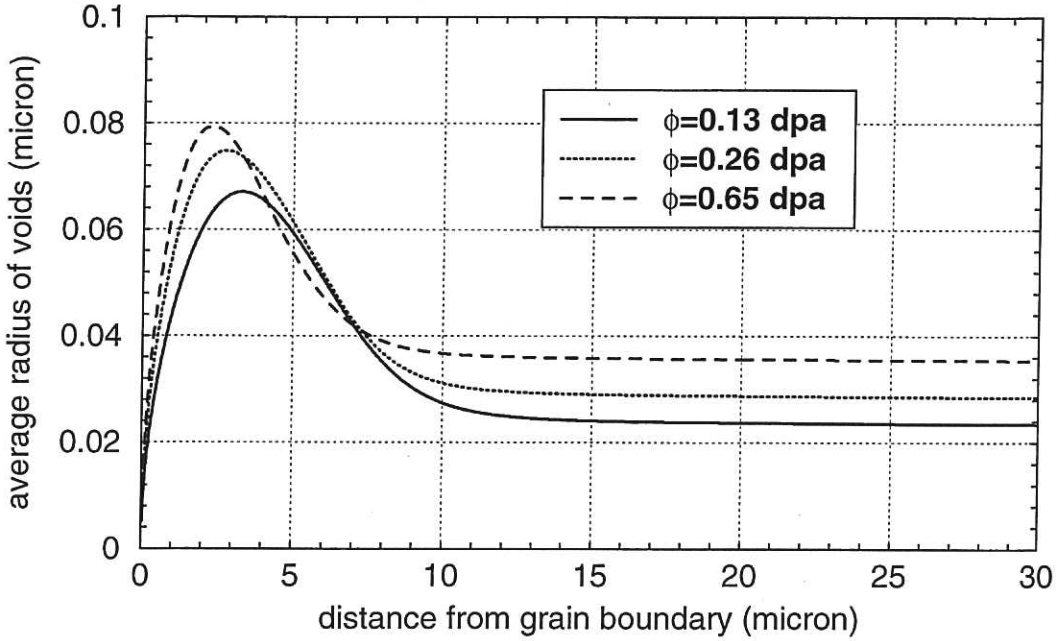

FIG. 6. Profiles illustrating the evolution of the average radius of growing voids considered as a function of the distance to the grain boundary. The average radius of the void $\langle a \rangle$ is defined as $\langle a \rangle = (3S_v/4\pi N_v)^{1/3}$, where S_v represents the local void swelling and N_v is the local volume density of voids. By comparing results shown in this figure with those shown in Fig. 3 we find that the density of voids in the region immediately adjacent to the grain boundary is substantially lower than that in the interior of the grain. At the same time the average size of voids growing near the boundary exceeds significantly the average size of voids growing in the interior region of the grain.

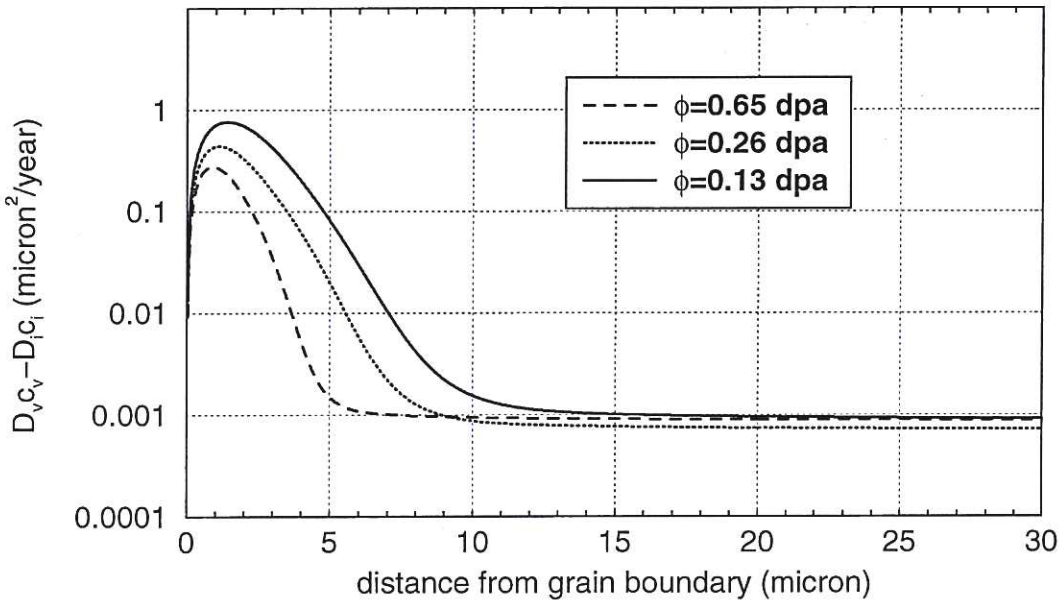

FIG. 7. This figure shows how the net vacancy flux to voids $D_v c_v - D_i c_i$ varies as a function of distance x to the grain boundary and as a function of irradiation dose. The peak of function $D_v c_v(x) - D_i c_i(x)$ in the vicinity of the grain boundary is associated with low total density of sinks in that region. The gradual drift of the peak of the void size profile towards the grain boundary visible in Figure 6 is related to the evolution of the profile of net vacancy flux shown in this figure.